

Optical transmission and photoluminescence of silicon nitride thin films implanted with Si ions

Ye, J. D.; Ding, Liang; Liu, Yang; Wong, Jen It; Fung, Stevenson Hon Yuen; Cen, Zhan Hong; Chen, Tupei; Liu, Zhen; Yang, Ming

2009

Ding, L., Ye, J. D., Liu, Y., Wong, J. I., Fung, S. H. Y., Cen, Z. H., et al. (2009). Optical transmission and photoluminescence of silicon nitride thin films implanted with Si ions. *Electrochemical and Solid State Letters*, 12(2), H38-H40.

<https://hdl.handle.net/10356/91848>

<https://doi.org/10.1149/1.3039952>

Electrochemical and Solid State Letters © copyright 2009 Electrochemical Society. This journal's website is located at

<http://scitation.aip.org/getabs/servlet/GetabsServlet?prog=normal&id=ESLEF6000012000002000H38000001&idty>

Downloaded on 28 Mar 2023 07:38:30 SGT



Optical Transmission and Photoluminescence of Silicon Nitride Thin Films Implanted with Si Ions

Z. H. Cen,^{a,z} T. P. Chen,^{a,z} L. Ding,^a J. D. Ye,^b Y. Liu,^a M. Yang,^a J. I. Wong,^a
Z. Liu,^a and S. Fung^c

^aSchool of Electrical and Electronic Engineering, Nanyang Technological University, 639798, Singapore

^bInstitute of Microelectronics, A*STAR, Science Park II, 117685, Singapore

^cDepartment of Physics, The University of Hong Kong, Hong Kong

The measurements of optical transmission, photoluminescence (PL), and PL excitation (PLE) of Si-implanted silicon nitride thin films annealed at various temperatures have been conducted. A red PL band at ~ 680 nm is largely enhanced by the Si implantation followed by thermal annealing. The excitation of the red PL band is attributed to the transitions between the Si-bond-related states of σ and σ^* , while the emission of the red PL band is believed to be from the radiative recombination associated with defect states which are largely increased by the Si ion implantation. Another excitation transition contributing to the red PL band, which is evidenced by the PLE peak at 425 nm, emerges after the annealing at 1100°C, and it is attributed to the formation of stable Si nanoclusters.

© 2008 The Electrochemical Society. [DOI: 10.1149/1.3039952] All rights reserved.

Manuscript submitted September 29, 2008; revised manuscript received November 10, 2008. Published December 4, 2008.

Recently, intensive research activities have been focused on the Si-rich silicon nitride (SRN) materials, which have not only lower injection barriers for electrons and holes compared with silicon oxide, but also the possibility to emit strong photons at the short wavelengths such as violet light.¹⁻⁴ The SRN could be a promising candidate for Si-based full-color light-emitting devices. Strong photoluminescence (PL) tunable from red to violet has been demonstrated in the SRN materials.^{2,3} However, the emission mechanism still remains controversial. The observed PL from the SRN materials was attributed to either the recombination at defect centers or the quantum confinement of silicon nanoparticles.^{2,4} Many techniques have been used to fabricate the SRN, such as chemical vapor deposition,¹⁻³ reactive evaporation,⁴ and sputtering.⁵ To the best of our knowledge, Si ion implantation, which has been successfully employed in fabrication of luminescent Si nanoparticles embedded in the silicon oxide matrix,^{6,7} was seldom used to synthesize the SRN.^{8,9} In addition, the optical properties of the SRN prepared by this technique have not been fully investigated. In this work, the PL, PL excitation (PLE), and optical transmission of silicon nitride thin films implanted with Si ions have been studied, and the annealing effect is examined also.

Silicon nitride films with a thickness of 120 nm were deposited by low-pressure chemical vapor deposition on either a quartz substrate or a 30 nm thick SiO₂ thin film thermally grown on Si(100) wafers. Si ions were implanted into the silicon nitride films at an energy of 30 keV at a dose of 3.5×10^{16} atoms/cm² at room temperature. The maximum volume fraction of the implanted Si is $\sim 21\%$ at a depth of 33 nm, as determined by the stopping and range of ion in matter (SRIM) calculation.¹⁰ Subsequently, the implanted films were thermally annealed in N₂ ambient at temperatures ranging from 800 to 1100°C for 1 h. PL spectra were taken with a commercial ACCENT RPM2000 PL system using an excitation laser of 325 nm line with a power of 1 mW. PLE measurements were carried out on a fluorescence spectrophotometer (Fluorolog-3, Jobin Yvon). UV-visible transmissions were measured in the wavelength range from 200 to 800 nm using a double-channel spectrophotometer (MPC-2200, Shimadzu). All spectral measurements were performed at room temperature.

Figure 1 shows the optical transmissions of the Si-implanted silicon nitride films grown on a quartz substrate and annealed at different temperatures. As shown in the figure, the Si ion implantation causes a reduction in the transmission as compared to the pure silicon nitride film, which could be attributed to the implantation-induced damages to the silicon nitride atom networks and the intro-

duction of excess Si ions. As can be seen in Fig. 1, thermal annealing leads to a partial recovery in the transmission, suggesting a partial recovery in the silicon nitride matrix or the defect passivation by the annealing.¹¹ The optical transmission spectra for the samples annealed below 1100°C are nearly identical, while the annealing at 1100°C yields a lower transmission compared with other annealing at lower temperatures, as presented in the inset of Fig. 1. These results suggest that the structure of the sample annealed at 1100°C is distinct from those of the samples annealed at lower temperatures and the difference might be due to the formation of stable Si nanoclusters in the 1100°C annealing.⁸ However, the evolution of the film structure with implantation and annealing should be reflected in the light emission properties, as discussed below.

The PL spectrum of the Si-implanted sample annealed at 1100°C is shown in Fig. 2. The PL from the control sample (i.e., without the Si ion implantation) is also included in the figure for comparison. Two emission bands located at ~ 435 nm (2.8 eV, the blue PL band) and ~ 680 nm (1.8 eV, the red PL band), respectively, can be observed for both samples, but the red light emission from the pure silicon nitride is much weaker as compared to that from the Si-

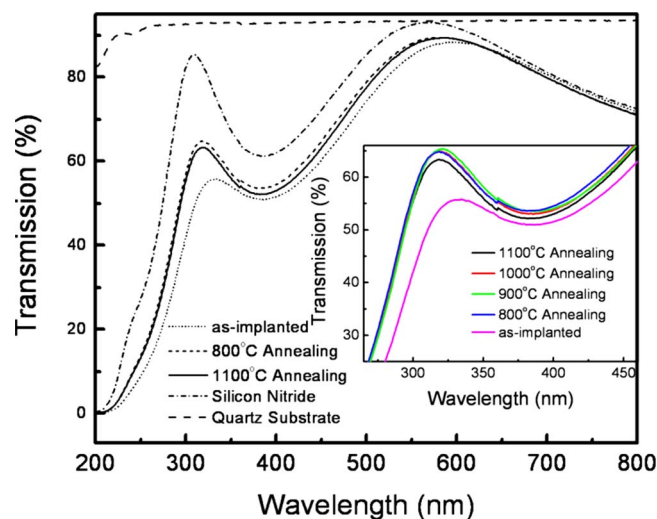


Figure 1. (Color online) Optical transmission spectra of the Si-implanted silicon nitride thin films grown on a quartz substrate and annealed at various temperatures. The optical transmission spectra of the quartz substrate and pure silicon nitride film grown on a quartz substrate are also included for comparison. The inset shows the scaled-up optical transmission spectra in the short-wavelength range.

^z E-mail: cen2001@ntu.edu.sg; echentp@ntu.edu.sg

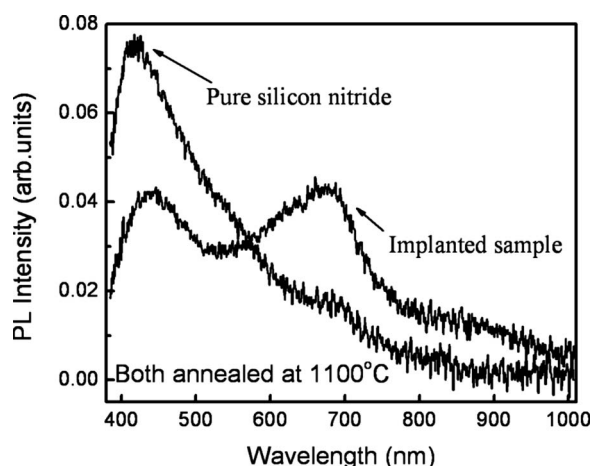


Figure 2. PL spectra of the Si-implanted silicon nitride and the pure silicon nitride thin film (i.e., the control sample), both annealed at 1100°C.

implanted sample. The blue PL band could be attributed to the radiative transition between the defect states related to the nitrogen dangling bonds.¹² Although this blue emission is believed to originate from the silicon nitride host matrix, it is also affected by the Si ion implantation. As shown in Fig. 2, the intensity of the blue PL band from the Si-implanted sample is obviously reduced with a broadened and redshifted peak as compared with that from the pure silicon nitride. This is similar to the situation of Ar⁺ ion implantation into silicon nitride.^{13,14}

Unlike the blue PL band, the red PL band is enhanced by the Si ion implantation. As can be seen in Fig. 2, the light emission at around 680 nm becomes much stronger due to the Si implantation. Although this red light emission has been observed from SRN materials in several studies,^{2,4,15,16} its origin is still controversial. It is often attributed to the recombination via the defect states,^{3,12,17} such as the Si-Si defects in the silicon nitride matrix,^{12,17} but some researchers also argued that it resulted from the quantum confinement of the Si nanoparticles in the host matrix.^{2,4,9,15,16}

As shown in Fig. 3, the red PL band cannot be observed in the as-implanted sample but it emerges after a thermal annealing. The nonradiative defect centers introduced by the ion implantation in the as-implanted sample can explain the absence of the red PL band. The elimination of these nonradiative defect centers by annealing, which is suggested by the optical transmission measurement, facilitates the light emission of the red and blue PL bands. When the annealing temperature is higher than 800°C, the light emissions of the two bands are quenched gradually in general, as summarized in the inset of Fig. 3. The quenching in PL is consistent with the observation reported in Ref. 3 that the PL from the SRN was weakened when the annealing temperature was increased from 700°C to a higher temperature. The evolution of the PL intensity with annealing

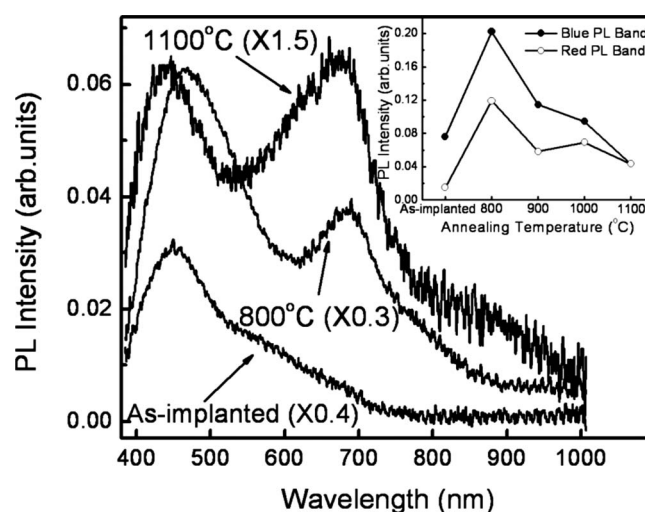


Figure 3. PL spectra of the Si-implanted silicon nitride thin films annealed at different temperatures. The inset shows the evolution of the PL intensity with the annealing temperature for the blue (435 nm) and red (680 nm) PL bands.

temperature, which can also be observed from the control samples, can be interpreted in terms of the nonradiative defects due to the hydrogen desorption.¹³ Interestingly, when the annealing temperature is increased from 800 to 1100°C, the quenching of the red PL band is slower than that of the blue PL band. For the 1100°C annealing, the red PL band has intensity as strong as the blue PL band, as shown in Fig. 2. Indeed, from the annealed sample with a thinner Si-implanted silicon nitride film, the red PL band is the major light emission, because the blue PL band originates from the silicon nitride host matrix as discussed above. There is no significant shift in the red PL band for different annealing temperatures, which is a characteristic of the defect-related PL.¹⁸

To further understand the red light emission, PLE measurements were conducted for all the samples. Figure 4 shows the PLE spectra monitored at 680 nm for the as-implanted and the annealed Si-implanted samples as well as the pure silicon nitride. To avoid the harmonic effect, the PLE signals at around 340 nm were not measured. There is no particular feature existing in the PLE spectra of the as-implanted sample and the control sample, being consistent with the observation of weak red PL bands in these samples. As can be seen in Fig. 4a, a broad PLE peak at around 290 nm can be observed for all the annealed samples. The onset wavelength of this PLE peak is ~310 nm (4 eV), which is close to the Tauc bandgaps (4.1 eV) of the annealed Si-implanted samples derived from the optical transmissions shown in Fig. 1. This PLE peak suggests that the major contribution for the red-band emission is the excitation

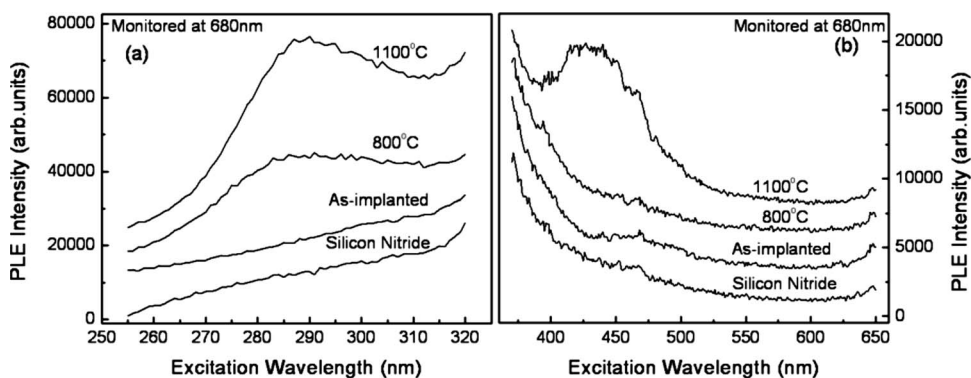


Figure 4. PLE spectra monitored at 680 nm of the Si-implanted samples annealed at different temperatures. The individual PLE spectrum is shifted along the vertical direction for a clear comparison.

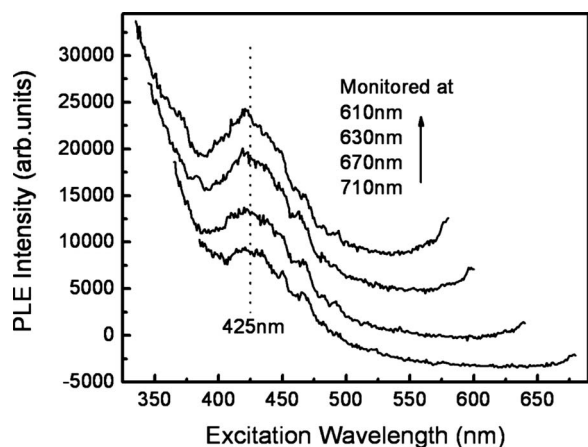


Figure 5. PLE spectra monitored at different wavelengths for the Si-implanted sample annealed at 1100°C. The individual PLE spectrum is shifted along the vertical direction for a clear comparison.

transition between the Si-bond-related states of σ and σ^* which are positioned near the valence and conduction band edges of silicon nitride, respectively.^{12,19}

The annealing at 1100°C gives rise to a remarkable PLE peak at around 425 nm (2.9 eV) which cannot be observed in other Si-implanted samples annealed at lower temperatures, as shown in Fig. 4b. The additional PLE peak indicates that the annealing at 1100°C introduces one more excitation transition for the red PL band.¹⁸ For the annealing at 1100°C, the emergence of the PLE peak at 425 nm coincides with the decrease in the optical transmission which has been attributed to the formation of stable Si nanoclusters. Therefore, the PLE peak at 425 nm could originate from the formation of stable Si nanoclusters also. Figure 5 shows the PLE spectra at various monitored wavelengths of the red PL band for the annealing at 1100°C. As can be seen in the figure, the PLE peak at \sim 425 nm is independent of the monitored wavelength. This is in contrast to the situation in which the PLE peak shifts toward a lower energy as the monitored wavelength is increased for the transitions associated with the quantum confinement effect.²⁰⁻²² Therefore, one may conclude that the quantum confinement effect does not play a dominant role in the red PL band in the present study. Comparing with the red PL band (at 680 nm), large Stokes shifts are observed for the two PLE peaks (i.e., at 290 and 425 nm, respectively). This implies that the PL primarily occurs via the relaxed radiative recombination states.²³ As the red PL band is strongly influenced by the Si implantation as shown in Fig. 2 and cannot be observed from the Ge-implanted silicon nitride films,¹⁴ it is reasonable to argue that the emission of the red PL band originates from the radiative recombination associated with the Si-related defect states, which are largely increased by the Si ion implantation.

In summary, PL from the silicon nitride films implanted with Si ions has been studied. The effects of the Si implantation and the

postimplant thermal annealing on the PL were examined. A red PL band at around 680 nm is enhanced by both the Si implantation and the subsequent thermal annealing, and the blue PL band originating from the silicon nitride host is also influenced by the implantation. Based on the results of PLE and optical transmission, the major excitation process for the red PL band is related to the transitions between the Si-bond-related states close to the silicon nitride band-edges. After the thermal annealing at 1100°C, one more excitation transition, which is evidenced by the PLE peak at 425 nm and is related to the formation of stable Si nanoclusters, contributes to the red PL band also. Both the PL and PLE results suggest that the emission of the red PL band originates from the radiative recombination associated with the Si-related defect states.

Acknowledgment

This work has been financially supported by the Ministry of Education Singapore under project ARC no. 1/04 and by the National Research Foundation of Singapore under project NRF-G-CRP 2007-01.

References

1. N. M. Park, C. J. Choi, T. Y. Seong, and S. J. Park, *Phys. Rev. Lett.*, **86**, 1355 (2001).
2. G. Y. Sung, N. M. Park, J. H. Shin, K. H. Kim, T. Y. Kim, K. S. Cho, and C. Huh, *IEEE J. Sel. Top. Quantum Electron.*, **12**, 1545 (2006).
3. L. Dal Negro, J. H. Yi, J. Michel, L. C. Kimerling, T.-W. F. Chang, V. Sukhovatkin, and E. H. Sargent, *Appl. Phys. Lett.*, **88**, 233109 (2006).
4. M. Molinari, H. Rinnert, and M. Vergnat, *J. Appl. Phys.*, **101**, 123532 (2007).
5. M. Vetter and M. Rojahn, *Mater. Sci. Eng., B*, **71**, 321 (2000).
6. L. Ding, T. P. Chen, Y. Liu, C. Y. Ng, and S. Fung, *Phys. Rev. B*, **72**, 125419 (2005).
7. Y. Liu, T. P. Chen, L. Ding, M. Yang, J. I. Wong, C. Y. Ng, S. F. Yu, Z. X. Li, C. Yuen, F. R. Zhu, et al., *J. Appl. Phys.*, **101**, 104306 (2007).
8. Z. H. Cen, T. P. Chen, L. Ding, Y. Liu, M. Yang, J. I. Wong, Z. Liu, Y. C. Liu, and S. Fung, *Appl. Phys. Lett.*, **93**, 023122 (2008).
9. Y. Y. Lü, C. L. Liu, L. J. Yin, Z. Wang, and X. D. Zhang, *Radiat. Meas.*, **43**, S594 (2008).
10. J. F. Ziegler, J. P. Biersach, and U. Littmark, *SRIM*, Pergamon, New York (2006); available from www.srim.org
11. L. Dal Negro, R. Li, J. Warga, S. Yerci, S. N. Basu, S. Hamel, and G. Galli, *Silicon Nanophotonics: Basic Principles, Present Status and Perspectives*, L. Khriachtchev, Editor, Chap. 12, World Scientific, River Edge, NJ (2008).
12. S. V. Deshpande, E. Gulari, S. W. Brown, and S. C. Rand, *J. Appl. Phys.*, **77**, 6534 (1995).
13. K. S. Seol, T. Futami, T. Watanabe, Y. Ohki, and M. Takiyama, *J. Appl. Phys.*, **85**, 6746 (1999).
14. I. E. Tyschenko, V. A. Volodin, L. Rebohle, M. Voelskov, and V. Skorupa, *Semiconductors*, **33**, 523 (1999).
15. H. L. Hao, L. K. Wu, W. Z. Shen, and H. F. W. Dekkers, *Appl. Phys. Lett.*, **91**, 201922 (2007).
16. M. Wang, D. Li, Z. Yuan, D. Yang, and D. Que, *Appl. Phys. Lett.*, **90**, 131903 (2007).
17. V. V. Vasilev and I. P. Mikhailovskii, *Phys. Status Solidi A*, **90**, 355 (1985).
18. H. Z. Song and X. M. Bao, *Phys. Rev. B*, **55**, 6988 (1997).
19. J. Robertson, *Philos. Mag. B*, **63**, 47 (1991).
20. Y. H. Xie, W. L. Wilson, F. M. Ross, J. A. Mucha, E. A. Fitzgerald, J. M. Macaulay, and T. D. Harris, *J. Appl. Phys.*, **71**, 2403 (1992).
21. M. V. Wolkin, J. Jorne, P. M. Fauchet, G. Allan, and C. Delerue, *Phys. Rev. Lett.*, **82**, 197 (1999).
22. Z. Y. Zhang, X. L. Wu, J. C. Shen, L. L. Xu, and P. K. Chu, *Appl. Phys. Lett.*, **91**, 193111 (2007).
23. R. Huang, K. Chen, B. Qian, S. Chen, W. Li, J. Xu, Z. Ma, and X. Huang, *Appl. Phys. Lett.*, **89**, 221120 (2006).